Algal Research 50 (2020) 101970

Contents lists available at ScienceDirect

Algal Research

journal homepage: www.elsevier.com/locate/algal

Evolutionary diverse *Chlamydomonas reinhardtii* Old Yellow Enzymes reveal distinctive catalytic properties and potential for whole-cell biotransformations

Stefanie Böhmer[a,1], Christina Marx[b,1], Álvaro Gómez-Baraibar[c], Marc M. Nowaczyk[d], Dirk Tischler[c], Anja Hemschemeier[a], Thomas Happe[a,*]

[a] Faculty of Biology and Biotechnology, Photobiotechnology, Ruhr University Bochum, Universitätsstr. 150, 44801 Bochum, Germany
[b] SolarBioproducts Ruhr, Business Development Agency Herne, Westring 303, 44629 Herne, Germany
[c] Faculty of Biology and Biotechnology, Microbial Biotechnology, Ruhr University Bochum, Universitätsstr. 150, 44801 Bochum, Germany
[d] Faculty of Biology and Biotechnology, Plant Biochemistry, Ruhr University Bochum, Universitätsstr. 150, 44801 Bochum, Germany

A B S T R A C T

Old Yellow Enzymes (OYEs) selectively reduce carbon-carbon double bonds of a broad range of substrates with excellent stereoselectivity. Current challenges of their application in bio-based industrial processes are the cost-efficient regeneration of the nicotinamide co-substrate and expanding the range of industrially relevant substrates. Microalgae represent a rich and mostly untapped source for OYEs with novel catalytic properties and are promising whole-cell factories that regenerate nicotinamide by photosynthesis. By comparative phylogenetics, we identified 20 putative OYEs in eleven algal species. Three recombinant OYEs from the unicellular green alga *Chlamydomonas reinhardtii* (CrOYEs) reveal diverse biocatalytic properties and potential for enzyme optimization. High substrate conversion activities of living algal wild type and mutant cells linked the biocatalytic profiles to *in vivo* functionality and demonstrate the potential of microalgae as sources for distinctive OYE activities and for light-driven biotransformations.

1. Introduction

The development of sustainable, or 'green', chemical processes represents one of the urgent tasks for building a future climate and environmentally friendly economy. Enzymes often excel chemical processes due to their high specificity and activity under ambient conditions, and they have already been employed in the industrial production of, for example, pharmaceuticals or flavors [1,2]. Challenges for a firm and broad establishment of bio-based processes in our industries are the extension of substrate scopes, the optimization of individual biocatalysts and the development of stable and efficient processes. Mining the enormous biodiversity of microorganisms is a promising strategy to identify novel enzymatic activities, whereas the use of whole-cell biocatalysis is a potential route towards self-regenerating sustainable processes [3].

Asymmetric alkene hydrogenations are widely used industrial reactions, because they result in the creation of up to two chiral carbon centers. Organic syntheses usually employ metal catalysts [e.g. [4,5]], often with a strong impact on economic and environmental aspects of the process. One example for substituting a synthetic process by biocatalysis is the production of enantiomerically pure (*R*)-citronellal, an industrially important terpene [6]. Technical methods employ different metal catalysts, often at elevated temperatures and in organic solvents [7,8], whereas a biocatalyst of the Old Yellow Enzyme (OYE) family can produce quite pure (*R*)-citronellal at ambient temperatures and in aqueous solution, employing an isomer mixture of the starting material, (*E/Z*)-citral [9]. OYEs are nicotinamide adenine dinucleotide (phosphate)- (NAD(P)H-) dependent oxidoreductases that commonly use a reduced flavin mononucleotide (FMN) cofactor for the stereo- and enantioselective reduction of α,β-unsaturated substrates through a bi-bi ping-pong mechanism (Fig. 1) [10–14]. FMN is reduced through hydride transfer from NAD(P)H, the costs of which are one of the hurdles for the commercial application of OYEs [e.g. [15]].

Since the discovery of the ene reductases of the OYE family in the 1930s, over 100 proteins of this family have been identified in diverse bacteria, fungi, cyanobacteria and plants [16–18]. These enzymes have been found to catalyze various reactions of industrial interest, and enzyme engineering approaches have resulted in biocatalysts optimized, for example, regarding enantioselectivity, which is of particular importance for the pharmaceutical industry [19–22]. Despite the high number of OYEs that have been characterized, the mining of increasingly available (meta-) genomic data for ene reductases with special

* Corresponding author.
E-mail address: thomas.happe@rub.de (T. Happe).
[1] Contributed equally to this work.

https://doi.org/10.1016/j.algal.2020.101970
Received 6 April 2020; Received in revised form 26 May 2020; Accepted 5 June 2020
Available online 17 June 2020

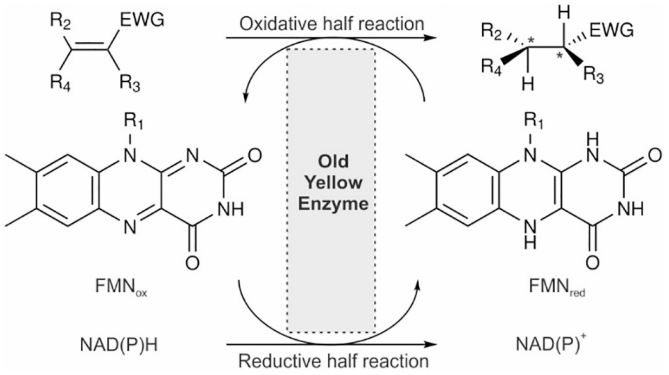

Fig. 1. Stereoselective reduction of an activated C = C double bond by an Old Yellow Enzyme (OYE, synonym: ene reductase). NAD(P)H acts as an electron donor to reduce the flavin cofactor FMN. The product contains up to two chiral centers. EWG: electron withdrawing group.

substrate scopes or characteristics optimal for industrial applications, such as temperature or solvent tolerance, promises to broaden the applicability of OYEs [e.g. [23]].

Although highly stable enzymes have been identified from extremophiles, the industrial use of most enzymes is still hampered by their limited long-term performance [24]. Employing living cells is one way of providing an inherent self-regenerating system. In case of OYE-catalyzed reactions, the metabolic recycling of reduced nicotinamide is an additional advantage, especially in photosynthetic organisms that harness light energy for the regeneration of NAD(P)H. For a long time, successful biotransformation in a sufficient scale by whole cells was only achieved using either bacteria, mostly *Escherichia coli*, or yeast as hosts. (2*R*,5*R*)-dihydrocarvone, for example, is a key intermediate in the synthesis of natural products and a chiral starting material for the synthesis of antimalarial drugs as recently summarized by Tischler et al., 2020 [25]. Its production was achieved by using an asymmetric whole-cell bioreduction system with recombinant *E. coli* overproducing an OYE from the cyanobacterium *Nostoc* sp. PCC 7120 [26]. In 2016, Köninger et al. reported a whole-cell biotransformation system of various alkenes using recombinant cyanobacteria expressing the OYE YqjM from *Bacillus subtilis* [27]. Results were comparable to *E. coli*-based systems, and the light reactions of photosynthesis were exploited as a recycling system for the costly co-substrate NADPH.

Here, we searched for OYEs in eukaryotic microalgae as these organisms, although offering a rich metabolic flexibility, have so far been underrepresented in the field of ene reductase research. These organisms are not only a promising source of novel OYEs, but might be harnessed for whole-cell bioreduction systems, their chloroplast offering a compartmentalized metabolic environment. Including 20 newly identified OYE sequences into an updated phylogenetic analysis led us to propose new subclasses within the OYE family. This finding is supported by the biochemical characterization of three novel algal OYEs from the unicellular green alga *Chlamydomonas reinhardtii*, one of which shows an unusual substrate scope and activity. Additionally, we were able to link the *in vitro* activity of the *C. reinhardtii* OYEs with *in vivo* biocatalysis by living algal cells. Our results suggest that green algae may be harnessed for sustainable photosynthetic *in vivo* biocatalytic applications.

2. Material and methods

2.1. Chemicals

All chemicals and substrates used for buffers and activity assays were purchased from Sigma-Aldrich (Steinheim, Germany), Carl Roth (Karlsruhe, Germany), Thermo Fisher (Kandel, Germany) and Merck Chemicals GmbH (Darmstadt, Germany) and of the purest grade available. 2-Methylmaleimide and 2-methylsuccinimide were synthesized as described previously [27].

2.2. Algal strains, standard growth conditions and cellular biotransformation assays

C. reinhardtii wild type CC-5325 (*cw15* mt–) and mutant strain *croye3* (LMJ.RY0402.159107; derived from strain CC-5325) from the Chlamydomonas Library Project (CLiP) [28], featuring an insertion of a paromomycin resistance cassette within gene *Cre17.g727300* (*NFO2*; named *CrOYE3* here), were obtained from the Chlamydomonas Resource Center (University of Minnesota, MN, USA). Liquid cultures were grown in 250 mL conical flasks in 50 mL Tris acetate phosphate (TAP) medium [29]. Growth occurred at 20 °C on a reciprocating shaker at 130 rpm with continuous bottom-up illumination (alternating one Osram Fluora and two Osram Lumilux CoolWhite light bulbs; 100 µmol photons × m^{-2} × s^{-1}). The insertion site of the paromomycin resistance cassette in gene *CrOYE3* in strain LMJ.RY0402.159107 was confirmed by PCR on genomic DNA isolated according to previous protocols [30]. PCR was performed using Phusion High-Fidelity DNA Polymerase (New England Biolabs, Ipswich, Massachusetts, USA) and oligonucleotides 7 to 10 (Table S1, Supporting Information), and the cassettes' flanking regions were sequenced.

The chlorophyll (Chl) content of algal cultures was determined by acetone extraction as described earlier [31]. For biotransformation assays, algal cells were grown to the mid to late exponential phase (10–20 µg Chl × mL^{-1}), harvested by centrifugation (201 × *g*, 20 °C, 3 min) and resuspended in fresh TAP medium to reach a Chl concentration of about 100 µg Chl × mL^{-1}. For each biotransformation assay, 10 mL of the concentrated cells were incubated under standard growth conditions as described above in 100 mL conical flasks in the presence of 1 mM substrate or product. Samples of 200 µL were taken after defined time points (15 min–24 h) and prepared for gas chromatography as described for enzyme assays below.

2.3. Cloning, heterologous production and purification of recombinant OYEs

C. reinhardtii cDNA was synthesized from total RNA extracted from strain CC-124. RNA isolation and DNase treatment was done as reported before [32]. Total cDNA was synthesized applying oligo(dT) primers and employing the Promega Kit GoScript Reverse Transcription System (Promega GmbH, Walldorf, Germany) according to the manufacturer's instructions. The coding sequences of the Old Yellow Enzyme family proteins CrOYE1-3 (*Cre01.g050150* (*NFO1*), named *CrOYE1* here; *Cre03.g210513*, named *CrOYE2*; *Cre17.g727300* (*NFO2*), named *CrOYE3* here) were then amplified using specific oligonucleotides with overhangs providing restriction sites for cloning (Table S1, Supporting Information). PCR products were first cloned into pJET1.2. After sequencing by the DNA sequencing service at the chair for biochemistry (Biochemistry I, Receptor Biochemistry, at Ruhr University Bochum, Germany), the sequences were cloned into vector pASK_IBA37 + (IBA Lifesciences, Göttingen, Germany) using *Eco*RI and *Nco*I restriction sites, resulting in plasmids pASK_IBA37 + _OYE1, pASK_IBA37 + _OYE2 and pASK_IBA37 + _OYE3. The Cys71Ser variant of CrOYE1 was generated by QuikChange™ site-directed mutagenesis of plasmid pASK_IBA37 + _OYE1, applying oligonucleotides 11 and 12 (Table S1, Supporting Information) and Phusion High-Fidelity DNA Polymerase (New England Biolabs) according to published protocols [33]. *B. subtilis* YqjM, amplified from *B. subtilis* genomic DNA, was expressed from plasmid pRSET (Thermo Fisher). Expression from both pASK-IBA37 + and pRSET results in proteins equipped with an N-terminal 6xHis-tag.

The generated plasmids were used for heterologous expression in *Escherichia coli* BL21 (DE3) Rosetta (F^- *ompT* $hsdS_B$ (r_B^- m_B^-) *gal dcm* (DE3) pRARE (Cam^R); Merck). Bacterial cells transformed with the

respective plasmids by electroporation were grown to an OD_{600} of 0.5 in 2 L conical flasks containing 500 mL LB-Lennox medium [34] supplemented with ampicillin (100 μg × mL^{-1}) and chloramphenicol (25 μg × mL^{-1}) at 37 °C and shaking at 180 rpm. Then, expression was induced by adding 0.05 μg × mL^{-1} anhydrotetracycline (pASK-IBA3 +) or 0.5 mM isopropyl β-D-1-thiogalactopyranoside (pRSET). Cells were harvested after incubation overnight in a WiseCube WIS-30 incubator (Witeg Labortechnik GmbH, Wertheim, Germany) at 18 °C and shaking at 130 rpm (orbital motion 25 mm), resuspended and washed once in buffer A (300 mM NaCl, 50 mM potassium phosphate, pH 7.5). Cells were disrupted by ultrasonication on ice (Branson Sonifier 250) (six cycles, 30 s each, output energy of 50%, breaks of 30 s). Cell debris was removed by ultracentrifugation (180,000 × *g*, 1 h, 4 °C, Ti70 rotor, L8-80M Beckman Coulter, Krefeld, Germany). The supernatant, containing the soluble proteins, was sterile-filtrated (0.2 μm Filtropur S, Sarstedt, Nümbrecht, Germany) and subjected to nickel affinity chromatography (cOmplete His-tag Purification Resin, Roche GmbH, Basel, Switzerland). The protein fractions were eluted by an imidazole gradient (20–500 mM), then pooled and desalted twice using desalting columns (PD-10 Columns, GE Healthcare, Solingen, Germany) according to the manufacturer's instructions. Recombinant YqjM eluates were incubated with 100 μM FMN on ice for 1 h before desalting.

The presence of the recombinant target proteins and protein masses were verified by sodium dodecyl sulfate-polyacrylamide gel electrophoresis (SDS-PAGE) and immunodetection using an anti-His-tag antibody (Penta-His HRP conjugate antibody from Qiagen, Hilden, Germany). Protein concentration was determined spectrophotometrically at λ = 280 nm applying the standard calculation (1 Abs = 1 mg × mL^{-1}) (Nanodrop ND-1000, Peqlab, VWR International GmbH, Darmstadt, Germany). The recombinant proteins were aliquoted and stored at −20 °C for up to two months.

2.4. Characterization of the flavin cofactor

The flavin content of recombinant CrOYE1-3 was determined spectrophotometrically from absorption scans (300–600 nm, 515 HPLC Pump and 2998 Photodiode Array Detector, Waters, Eschborn, Germany). Flavin was extracted from purified protein samples (1–3 mg × mL^{-1}) by incubation for 20 min at 95 °C and subsequent centrifugation. The supernatant was analyzed by reverse phase- (RP-) HPLC (LC Column HyperClone 5 μm ODS (C18) 120, 250 × 4.6 mm, Phenomenex, Aschaffenburg, Germany) conducted at room temperature. A constant flow of 50 mM sodium acetate buffer, pH 5.0, containing 30% methanol was used for a 60 min runtime. A standard solution containing 0.1 mM flavin adenine dinucleotide (FAD) (retention time (RT): ~12 min), 0.1 mM FMN (RT: ~15 min) and 0.5 mM riboflavin (RT: ~28 min) in 50 mM potassium phosphate buffer, pH 7.5, was used and compared to the spectra of the CrOYE1-3 protein samples at the selected wavelength of 374 nm.

2.5. Determination of in vitro enzyme activity

For determining substrate scopes, stock solutions of 200 mM for each substrate and product in either the indicated reaction buffer or ethanol were utilized. *In vitro* activity assays using purified recombinant CrOYE1-3 were performed in a 1.5 mL scale in 1.5 mL micro reaction tubes. The standard reaction was carried out in 50 mM Tris-HCl buffer (pH 7.5) at 30 °C, shaking at 300 rpm in a thermal shaker (ThermoMixer® C, Eppendorf AG, Hamburg, Germany). Each sample contained 0.02–2 μM enzyme (provided by adding maximally 30 μL of the enzyme solutions), 3 μM FMN and 0.01–10 mM substrate. As reducing equivalents, either 1–3 mM NADPH were added or a glucose-6-phosphate dehydrogenase recycling system was used as described earlier (0.8 U glucose-6-phosphate dehydrogenase, 1–3 mM glucose-6-phosphate, 1 mM $NADP^+$) [12]. Samples of 200 μL were taken after 1–10 min, quenched by 2 μL concentrated hydrochloric acid and extracted with ethyl acetate (2:3) containing *n*-octanol as internal standard. The extracts were freed from water using $MgSO_4$ and then subjected to gas chromatography (GC-2010 Plus equipped with an autosampler AOC-20I and a barrier ion discharge ionization detector (BID) from Shimadzu Europe, Duisburg, Germany) using a chiral column (Hydrodex β-6TBDM from Macherey-Nagel GmbH & Co. KG, Düren, Germany) and helium as carrier gas. All calibration curves were linear in the range of substrate and product detection. More detailed information on the applied GC methods are listed in Table S2, Supporting Information. Stereoselectivity regarding the conversion of (*R*)-carvone to both possible diastereomers (2*S*,5*R*)- or (2*R*,5*R*)-dihydrocarvone was determined and calculated according to Tischler et al., 2020 [25].

Michaelis-Menten constants (K_m) and maximal reaction velocities (V_{max}) were determined for *N*-methylmaleimide by gas chromatography and for NADPH *via* spectrophotometric measurements (see below). In each case, the second substrate was kept in excess. For determining kinetic parameters for NADPH, NMI was always present at a concentration of 10 mM, and for those of NMI, NADPH was present at 1 mM and constantly enzymatically recycled (see above). K_m and V_{max} were obtained from non-linear regression of Michaelis-Menten plots using Microsoft Excel. Specific activities were calculated from product formation measured by GC, or, in the few cases where no product standard was available, from substrate consumption.

Temperature dependent activity was measured at standard conditions using 1 mM *N*-methylmaleimide (NMI). Reaction assay solutions were pre-incubated for 10 min at the target temperature prior to adding enzyme. Reaction velocities were determined after 3 min, which was in the linear reaction velocity range. For thermal stability measurements, 1.5 mL of enzyme diluted to the desired concentration in 50 mM Tris-HCl (pH 7.5) was incubated at temperatures between 30 and 70 °C. At defined times, enzyme samples were taken, and standard reactions were performed at 30 °C to determine the residual activity.

For determining the inactivation effect of NMI on CrOYE1-3 and YqjM, the reaction assays, including enzyme and 1 mM NMI, were pre-incubated for defined time intervals (0–120 min) at 30 °C. Then, standard reactions were performed by adding NADPH as a starting agent.

2.6. Spectrophotometric activity assays

For the determination of NADPH affinities and pH optima, a UV–Vis spectrometric assay using a V-750 spectrophotometer (JASCO Deutschland GmbH, Pfungstadt, Germany) was employed to monitor NADPH consumption at either 340 or 380 nm [35,36]. Control reactions without enzymes were performed to monitor enzyme-independent NADPH or substrate consumption, which was never observed. Samples were prepared in quartz cuvettes and preheated to 30 °C prior to measurement. Each sample contained 2–200 nM enzyme, 10 mM *N*-methylmaleimide as model substrate and 10 μM FMN in a total volume of 1 mL 50 mM Tris-HCl buffer (pH 7.5). For NADPH affinity measurements, the NADPH concentration was varied (0–1 mM). For pH optimum determination, the Tris-HCl buffer was substituted by a 50 mM Britton-Robinson buffer covering a pH range of 5–10 [18,37] and the samples contained 500 μM NADPH. Reactions were started by enzyme addition and the initial activity was monitored for 60 s. Each sample was prepared and measured in triplicate and the linear slopes of the reactions were determined with the Spectra Manager II Software (JASCO Deutschland GmbH, Pfungstadt, Germany). Activities were determined using a Lambert-Beer equation with suitable extinction coefficients (ε_{340} = 6.22 mM^{-1} cm^{-1}, ε_{380} = 1.23 mM^{-1} cm^{-1}).

2.7. Phylogenetic analysis

Genome annotations (listed in Table S3, Supporting Information) from Phytozome, picoPlaza and the National Center for Biotechnology Information (NCBI) were analyzed regarding the presence of putative

OYE encoding sequences in algae. First, previously published sequences of three OYEs, namely YqjM (*B. subtilis*), OPR3 (*Solanum lycopersicum*) and OYERo2 (*Rhodococcus opacus* 1CP) [35,38,39], were used as queries to interrogate the respective genomes employing the integrated BlastP analysis tools of the databases. Then, hit sequences were counter-analyzed using the BlastP and Conserved Domain Database search on NCBI, applying *E*-value thresholds of $< 1E^{-4}$ [40]. Sequence alignment of selected sequences (Table S3, Supporting Information) was done by ClustalW [41]. The evolutionary history was inferred by using the Maximum Likelihood method based on the JTT matrix-based model [42]. Initial trees for the heuristic search were obtained automatically by applying Neighbor-Join and BioNJ algorithms to a matrix of pairwise distances estimated using a JTT model, and then selecting the topology with superior log likelihood value (−20,001.37). Evolutionary analyses were conducted in MEGA7 [43]. The assignment of subclasses was based on a previous phylogenetic study [14], but was refined by distinguishing subclasses.

3. Results

3.1. Annotation and phylogeny of novel algal OYEs

The continuing identification of OYEs from diverse species resulted in constantly revised phylogenetic classifications [14,17,35,44,45]. Since algal OYEs have been underrepresented so far, we mined the algal and plant comparative genomic platforms picoPlaza and Phytozome and were able to identify 20 putative OYEs in eleven algal species (Table S3, Supporting Information).

A phylogenetic analysis of these 20 OYEs with a set of 77 OYE sequences from higher plants, bacteria and fungi resulted in a dendrogram based on, but refining the classification from Scholtissek et al. [14] (Fig. 2). The subclasses Ia, Ib and Ic identified here correspond to the former OYE subclass designated as 'classical' OYEs from plants and bacteria (referred to as class I in [14]). However, it became evident that this group needed to be separated into at least three subclasses (Ia-c), from which Ic seems not well defined yet and needs further attention. The previously described subclasses II and III are similar in both dendrograms and encompass 'classical' OYEs from fungi (formerly designated as class II) and 'thermophilic-like and mesophilic' OYEs originating from bacteria (formerly designated as class III) (Fig. 2) [14]. However, several putative algal OYEs cluster with bacterial enzymes in subclass III, so that a revision of the naming is recommended. Furthermore, three new subclasses were calculated in the analysis presented here, which also contain putative OYEs from both pro- and eukaryotes (Fig. 2). We noted that several algal species possess more than one putative OYE, some of which cluster with different subclasses. For example, *Ectocarpus siliculosus*, a filamentous brown alga, has three putative OYEs, of which EsOYE1 and EsOYE2 are placed in subclass Ic, whereas EsOYE3 can be found in subclass V (Fig. 2). The diatom *Phaeodactylum tricornutum* possesses two putative OYEs, which cluster with subclass Ic (PtOYE1) and subclass V (PtOYE2). The genome of the unicellular green alga *C. reinhardtii* contains four genes encoding putative OYEs, which were grouped in subclass Ib (Cre03.g2105133 and Cre03.g209393, which we named CrOYE2 and CrOYE4 here), subclass III (Cre01.g050150, alias NFO1, which we refer to as CrOYE1), and as an outlier between subclasses Ic and II (Cre17.g727300, alias NFO2, termed CrOYE3 here) (Fig. 2).

The comparably high number of putative OYEs in this microalgal species and their distribution over the phylogenetic tree, whose subclasses have been associated with different biochemical properties [14], suggested specialized activities and/or physiological functions, so that we chose a member of each of the different subclasses (CrOYE1, −2

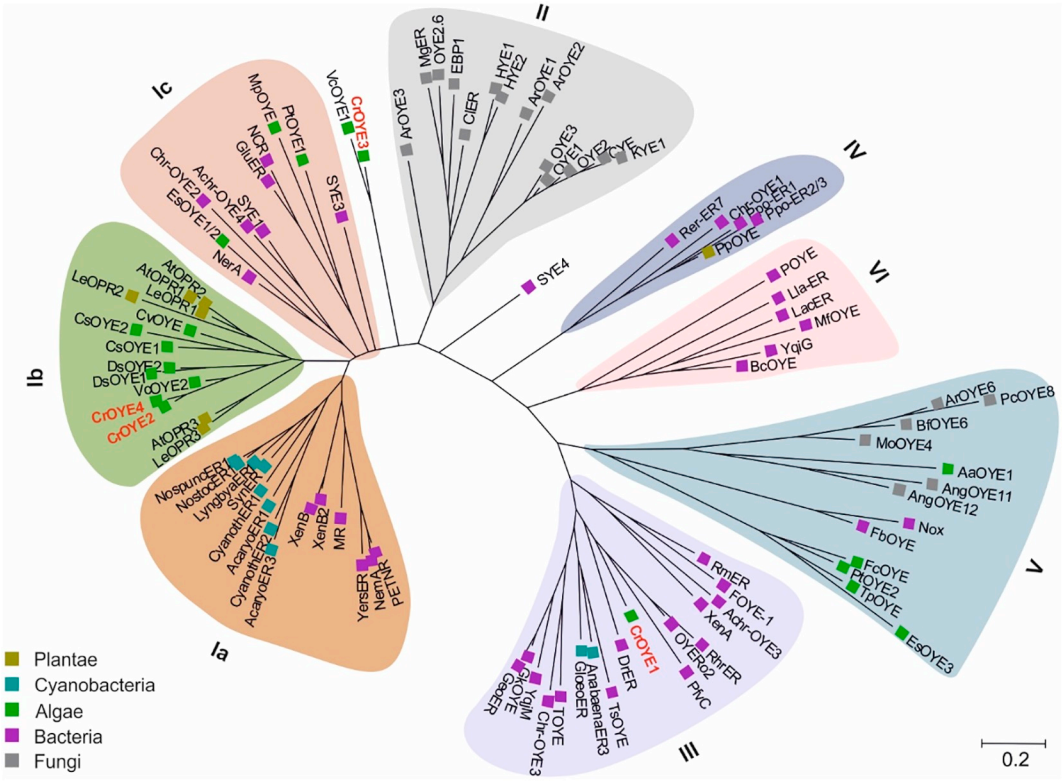

Fig. 2. Phylogenetic analysis of algal and previously described Old Yellow Enzymes (OYEs). The evolutionary history conducted in MEGA7 was inferred by using the Maximum Likelihood method based on the JTT matrix-based model. The tree with the highest log likelihood (−20,001.37) is shown. Proteins are labeled regarding their origin (higher and lower plants, olive; cyanobacteria, blue; algae, green; bacteria, purple; fungi, gray) and are listed in Table S3, Supporting Information. OYEs from *C. reinhardtii* are written in red letters. Branch lengths indicate the number of substitutions per site. (For interpretation of the references to color in this figure legend, the reader is referred to the web version of this article.)

and −3) for biochemical, and, in case of CrOYE3, physiological analyses.

3.2. Recombinant CrOYEs exhibit varying substrate scopes and reaction parameters

The coding regions for CrOYE1-3 were amplified from *C. reinhardtii* CC-124 wild type cDNA, and sequencing showed that, despite the presence of thousands of single nucleotide polymorphisms in different *C. reinhardtii* laboratory strains [e.g. [46]], they corresponded exactly to the coding sequences annotated on Phytozome v12, *Chlamydomonas reinhardtii* v5.5, based on strain CC-503. All three proteins are predicted to possess N-terminal chloroplast targeting sequences by the subcellular localization prediction tools PredAlgo, WoLF PSORT and ChloroP [47–49], the coding sequences of which were included in the recombinant proteins.

After heterologous expression in *E. coli*, CrOYE1-3 proteins were obtained in the soluble form with a yield of about 40 mg × L^{-1} bacterial culture. Affinity-purified proteins were analyzed by sodium dodecyl sulfate–polyacrylamide gel electrophoresis (SDS-PAGE) and anti-His-tag immunoblotting and revealed the expected calculated sizes of 48 kDa (CrOYE1), 49 kDa (CrOYE2) and 44 kDa (CrOYE3). Purified CrOYE1-3 showed a bright yellow color, indicative for a tightly bound flavin cofactor. The type of flavin cofactor was identified as FMN for all three enzymes using RP-HPLC (Fig. S1, Supporting Information).

In order to investigate enzymatic characteristics and the substrate scope of the CrOYE proteins a range of 14 unsaturated ketones including cyclic ketones, maleimides and other typical industrial compounds was employed. All substrates and products were subjected to gas chromatographic (GC) analysis and quantified. Specific activities and turnover frequencies were calculated from either product formation or substrate consumption (Table 1). Control incubations without enzymes were performed and resulted in no significant substrate degradation or conversion. 3-Methylated cyclic ketones (3-methyl-2-cyclohexen-1-one (3CH) and 3-methyl-2-cyclopenten-1-one (3CP)) as well as isophorone (IP) were not converted by any of the enzymes (Table 1). The only substrates that were converted by all three CrOYEs were the differently methylated maleimides (maleimide (MI), 2-methylmaleimide (2MI) and *N*-methylmaleimide (NMI)). CrOYE1 and CrOYE2, but not CrOYE3 converted the other substrates, whereas we did not find a non-maleimide substrate for CrOYE3 (Table 1). CrOYE1 and CrOYE2 showed an overall higher activity for maleimides, followed by the cyclic hexenones (2-cyclohexen-1-one (CH), 2-methyl-2-cyclohexen-1-one (2CH), 2-cyclopenten-1-one (CP)) and carvones (Table 1). Overall, CrOYE1 and CrOYE2 showed very similar activities for most of the substrates (Table 1). Also, both showed similar stereoselectivity for the conversion of (*R*)-carvone (CrOYE1: 93.0 ± 0.3% and CrOYE2: 92.2 ± 3.2% regarding (2*S*,5*R*)- over (2*R*,5*R*)-dihydrocarvone). Exceptions were cinnamaldehydes and 4-ketoisophorone (KIP). Whereas CrOYE1 converted α-methyl-*trans*-cinnamaldehyde (MTC) about threefold faster than CrOYE2, CrOYE2 showed a higher activity for the non-methylated form, *trans*-cinnamaldehyde (TC), and for KIP (Table 1).

All three enzymes displayed the highest activity towards *N*-methylmaleimide (NMI), and CrOYE3 stood out in that its activity of approximately 225 U × mg^{-1} was about 20-fold higher than those determined for CrOYE1 and CrOYE2 (Table 1). In summary, CrOYE1 and CrOYE2 showed a similar broad substrate scope, whereas CrOYE3 converted maleimide substrates only, but with notably high activities.

Optimum reaction temperatures and pH values were investigated using NMI as model substrate. The optimum reaction temperature for all three enzymes was 40 °C (Fig. S2a, Supporting Information). Note that standard reactions were conducted at 30 °C due to the temperature-dependent half-lives, which were roughly 5-fold longer at 30 °C (CrOYE1: 28 ± 8 days, CrOYE2: 27 ± 2 days, CrOYE3: 6 ± 0.1 days) than at 40 °C (CrOYE1: 5.7 ± 0.1 days, CrOYE2: 5.6 ± 0.8 days, CrOYE3: 1.9 ± 0.2 days). Varying pH optima were observed for the three recombinant enzymes (Fig. S2b, Supporting Information). The activity of CrOYE1 was highest between pH 5 and pH 7 and decreased steadily towards the more alkaline range. CrOYE2, in contrast, showed a constant activity over a broader range, namely from pH 5 to pH 9 and was inactive only thereafter. CrOYE3 featured the narrowest pH optimum range and was most active between pH 7.5 and pH 8 (Fig. S2b, Supporting Information).

3.3. Kinetic parameters and the inhibitory effect of maleimide differ between the three CrOYE proteins

Steady-state kinetics and Michaelis-Menten regressions (Fig. S3, Supporting Information) were employed to determine kinetic parameters for the CrOYE1-3 proteins (Table 2). CrOYE2 and CrOYE3 exhibited lower K_m values for NADPH (19.6 ± 0.1 μM and 84.9 ± 9.3 μM, respectively) than for NMI (346 ± 101 μM and 2643 ± 287 μM, respectively). CrOYE1, in contrast, had a lower K_m value for NMI of 73 ± 20 μM than for NADPH of 110.5 ± 43 μM (Table 2). Consistent with the results of the substrate scope assays described above, using NMI as a substrate, CrOYE3 yielded a remarkably high specific activity, which was approximately 20-fold higher than the maximum velocities of CrOYE1 and CrOYE2 (Table 2). Notably, however, CrOYE3 had a quite low affinity towards NMI with a K_m value of about 2600 μM, resulting in a much lower catalytic efficiency for NMI than for NADPH (Table 2). The diverse kinetic parameters of CrOYE1-3 using NMI as a substrate suggested that they might react differently in long-term assays using maleimides as substrates. Maleimides tend to react with cysteine residues in enzymes, thereby potentially inactivating them irreversibly, which results in decreased activity of OYE proteins over time [50]. In the ene reductase OYERo2a, a stability-improved variant of OYERo2 from *Rhodococcus opacus* [35], cysteine residue 25, which is only strongly conserved in subclass III OYEs [14], is responsible for the inhibitory effect of NMI, as revealed by the loss of inhibition in protein variants in which this residue was exchanged [50]. Because inhibition by maleimides may comprise a bottleneck for industrial biocatalyses, CrOYE1-3, each containing various cysteine residues, as well as the subclass III OYE YqjM from *B. subtilis*, having two cysteines, were incubated with the model substrate NMI, but without the NADPH co-substrate, for varying periods of time, and the remaining activity was then monitored upon addition of NADPH (Fig. 3a). CrOYE1, bearing a cysteine residue at position 71, conserved to that attacked by NMI in OYERo2a (Fig. 3b), indeed lost activity upon incubation with NMI. In contrast, a CrOYE1 protein variant, in which this residue was exchanged by serine, as well as CrOYE2, not featuring the conserved cysteine, but a threonine residue, remained active (Fig. 3a).

An additional effect of the C71S exchange in CrOYE1 was an increased initial velocity of 15.5 ± 0.2 U × mg^{-1} compared to 6.5 ± 0.5 U × mg^{-1} determined for the wild type form of the protein. Notably, CrOYE3, which, like CrOYE2, contains a threonine instead of a cysteine at the equivalent position (Fig. 3b), lost activity equally fast as YqjM (Fig. 3a).

3.4. Biotransformation of model substrates by whole algal cells

In view of the broad substrate scope of the CrOYE proteins the potential of *C. reinhardtii* cells as whole-cell biocatalysts was tested. Selected substrates that were previously converted by the recombinant algal OYEs *in vitro* were applied to living *C. reinhardtii* cells and both substrate consumption and product formation could be demonstrated (Fig. S4, Supporting Information). All tested substrates were indeed consumed to about 80–90%. Control incubations of substrates and products in cell-free culture medium resulted in no conversion.

Besides product and remaining substrate peaks, we observed additional peaks in the GC chromatograms occurring in whole-cell catalysis that were not detected *in vitro* (Fig. S4, Supporting Information). These

Table 1
Substrate scope of CrOYEs at standard reaction conditions (50 mM Tris-HCl pH 7.5, 30 °C, 300 rpm, 5 mM substrate). Velocities were calculated from either product formation or substrate consumption (= *), determined by GC. n.d.: no activity was detected. The experiments were done at least in biological triplicates.

Substrate				CrOYE		
Structure	Name	Acronym	Specific activity	1	2	3
	2-Cyclohexen-1-one	CH	[U × mg^{-1}]	6.2 ± 0.3	6.0 ± 0.2	n.d.
			[s^{-1}]	5.0 ± 0.2	5.0 ± 0.1	n.d.
	2-Methyl-2-cyclohexen-1-one	2CH	[U × mg^{-1}]	2.6 ± 0.1	2.7 ± 0.1	n.d.
			[s^{-1}]	2.0 ± 0.1	2.2 ± 0.1	n.d.
	3-Methyl-2-cyclohexen-1-one	3CH	[U × mg^{-1}]	n.d.	n.d.	n.d.
			[s^{-1}]	n.d.	n.d.	n.d.
	2-Cyclopenten-1-one	CP	[U × mg^{-1}]	1.7 ± 0.05	2.1 ± 0.2	n.d.
			[s^{-1}]	1.3 ± 0.1	1.7 ± 0.2	n.d.
	3-Methyl-2-cyclopenten-1-one	3CP	[U × mg^{-1}]	n.d.	n.d.	n.d.
			[s^{-1}]	n.d.	n.d.	n.d.
	Maleimide	MI	[U × mg^{-1}]	3.4 ± 0.3	5.8 ± 0.5	8.1 ± 1.1
			[s^{-1}]	2.8 ± 0.3	4.8 ± 0.4	6.0 ± 0.8
	2-Methylmaleimide	2MI	[U × mg^{-1}]	7.4 ± 0.01	7.6 ± 0.1	1.1 ± 0.1
			[s^{-1}]	5.9 ± 0.01	6.4 ± 0.1	0.8 ± 0.04
	*N*-Methylmaleimide	NMI	[U × mg^{-1}]	12.4 ± 0.3	9.2 ± 0.2	224 ± 30
			[s^{-1}]	9.9 ± 0.3	7.6 ± 0.1	165 ± 21
	Isophorone	IP	[U × mg^{-1}]	n.d.	n.d.	n.d.
			[s^{-1}]	n.d.	n.d.	n.d.
	4-Ketoisophorone*	KIP*	[U × mg^{-1}]	0.7 ± 0.1	2.5 ± 0.2	n.d.
			[s^{-1}]	0.6 ± 0.1	2.1 ± 0.2	n.d.
	(*R*)-Carvone	RC	[U × mg^{-1}]	2.3 ± 0.1	2.3 ± 0.1	n.d.
			[s^{-1}]	1.8 ± 0.1	1.9 ± 0.1	n.d.
	(*S*)-Carvone	SC	[U × mg^{-1}]	1.9 ± 0.01	2.2 ± 0.03	n.d.
			[s^{-1}]	1.5 ± 0.01	1.8 ± 0.03	n.d.
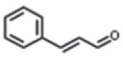	*trans*-Cinnamaldehyde	TC	[U × mg^{-1}]	0.2 ± 0.01	2.0 ± 0.1	n.d.
			[s^{-1}]	0.1 ± 0.01	1.7 ± 0.1	n.d.
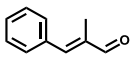	α-Methyl-*trans*-cinnamaldehyde*	MTC*	[U × mg^{-1}]	3.4 ± 0.03	1.2 ± 0.1	n.d.
			[s^{-1}]	2.8 ± 0.02	1.0 ± 0.1	n.d.

peaks were also observed when the algal cells were incubated with the respective products, indicating that they derived from downstream reactions. In order to analyze whether reactions took place extracellularly, supernatants of the *in vivo* reactions were sampled and analyzed. Neither substrate nor product peaks besides the internal standard signal were detectable in these. The substrates (*R*)-carvone (RC), (*S*)-carvone (SC), 2-cyclopenten-1-one (CP), 2-cyclohexen-1-one (CH) and *trans*-cinnamaldehyde (TC) were converted by the *C. reinhardtii* wild type strain CC-5325 with similar rates of about 65 µM × h^{-1} (Fig. 4). The stereoselectivity for the conversion of (*R*)-carvone of 96.9 ± 0.14% ((2*S*,5*R*)- over (2*R*,5*R*)-dihydrocarvone) was very similar to the respective values calculated for CrOYE1 and CrOYE2. Notably, *N*-Methylmaleimide (NMI) was converted approximately eightfold faster (540 ± 1.4 µM × h^{-1}). Because CrOYE3 showed the highest NMI *in vitro* conversion rate of the three analyzed enzymes, we applied NMI on a *croye3* mutant strain from the CLiP library [28], in which the disruption of gene *Cre17.g727300* by a paromomycin resistance cassette was confirmed by PCR and sequencing before (Fig. S5, Supporting Information).

The *C. reinhardtii croye3* mutant still converted NMI, but with a rate of 26 ± 4.5 µM × h^{-1}, NMI conversion by the mutant was significantly slower than by the wild type (540 ± 1.4 µM × h^{-1}) (Fig. 5a). We also noted that the *croye3* cells turned brownish after 22 h of incubation with NMI, whereas the wild type was still green (Fig. 5b).

Table 2
Kinetic parameters of CrOYEs regarding the co-substrate NADPH and NMI as a model substrate. The second substrate was always kept in excess (10 mM NMI for the determination of kinetic parameters for NADPH, and 1 mM NADPH, constantly enzymatically recycled, for analyzing NMI-related values). Maximum velocity V_{max}, Michaelis-Menten constant K_m, turnover frequency k_{cat} and catalytic efficiency k_{cat}/K_m were determined from Michaelis-Menten regressions of triplicates (Fig. S3, Supporting Information).

Enzyme	Substrate	V_{max} [U × mg^{-1}]	K_{cat} [s^{-1}]	K_m [μM]	k_{cat}/K_m [μM^{-1} × s^{-1}]
CrOYE1	NADPH	10.2 ± 0.6	8.1 ± 0.5	110.5 ± 43	0.08 ± 0.03
	NMI	6.9 ± 0.3	5.5 ± 0.2	73 ± 20	0.08 ± 0.02
CrOYE2	NADPH	11.2 ± 0.1	9.3 ± 0.04	19.6 ± 0.1	0.48 ± 0.02
	NMI	13.5 ± 1	11.2 ± 0.9	346 ± 101	0.035 ± 0.01
CrOYE3	NADPH	346.5 ± 15	254 ± 11	84.9 ± 9.3	3.02 ± 0.23
	NMI	337 ± 19	281 ± 16	2643 ± 287	0.12 ± 0.01

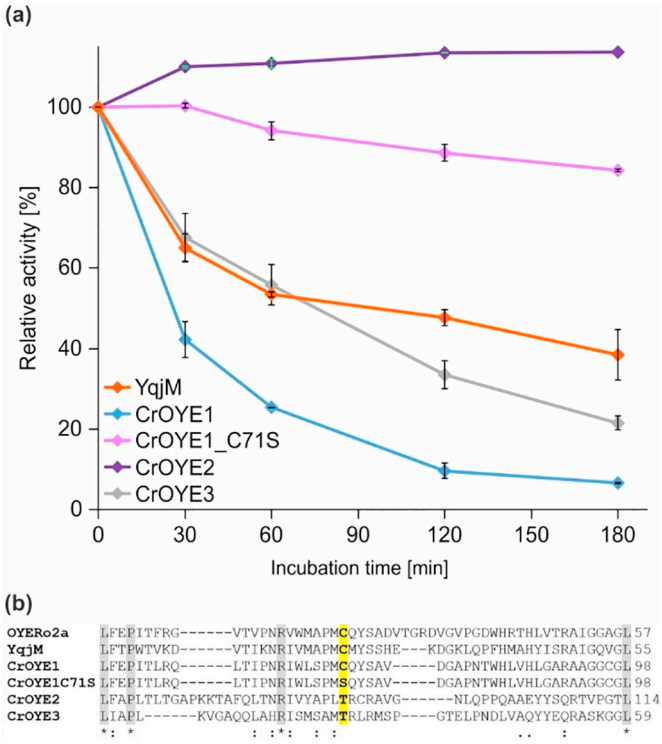

Fig. 3. Time-dependent inactivation of YqjM, CrOYE1-3 proteins and a CrOYE1 C71S variant upon pre-incubation with *N*-methylmaleimide (NMI). (a): Relative activity is plotted against the time of pre-incubation of each enzyme in a reaction assay with 1 mM NMI, but without NADPH, at 30 °C. At selected time points, the enzymatic reactions were started by adding 2 mM NADPH. After 1 to 3 min of incubation, samples were processed, and product formation was analyzed by GC. Controls without pre-incubation with NMI were performed and resulted in no significant loss of enzyme activity. The experiments were done in biological triplicate. Data points show the mean values, error bars indicate the standard deviation. (b): ClustalW alignment of OYERo2a, YqjM, CrOYE1–3 and a C71S variant of CrOYE1. The amino acid sequences surrounding the NMI-attacked Cys25 from OYERo2a are shown. Highly conserved residues are shaded in gray and indicated by asterisks, conservation of residues with highly similar properties are labeled by a colon, and conservation of amino acids with weakly similar features by a period. The cysteine residue targeted by NMI in OYERo2a and exchanged to serine (C71, CrOYE1-numbering) in CrOYE1 is highlighted in yellow.

Both the wild type and the *croye3* mutant were also tested for (*R*)-carvone conversion, for which no difference in substrate uptake or product formation were observed.

4. Discussion

4.1. Algae possess OYEs from diverse phylogenetic subclasses

Ene reductases of the Old Yellow Enzyme family are already utilized successfully in biotechnological processes, especially if enantiomerically pure compounds are required [9,22,26]. Yet, widening the spectrum of OYEs by representatives showing different substrate scopes and/or distinctive stability characteristics will be important to allow a broad applicability in the chemical and pharmaceutical industry. Tapping into the huge biodiversity potential provided by organisms with specialized metabolic competences promises to detect ene reductases with advantages for specific industrial processes. Here, we targeted the group of algae, a phylogenetically diverse group of organisms carrying out oxygenic photosynthesis, and identified 20 putative OYE homologues, which were not included in previous phylogenetic studies [14,17]. The inclusion of the algal sequences resulted in a dendrogram featuring a revised constellation of subgroups. Green algae, evolutionary ancestors of higher plants, predominantly possess OYEs from subclass Ib, in which plant OYEs can be detected too, suggesting an evolutionary relationship of these enzymes. In general, however, algal OYEs were grouped in quite diverse subclasses, which were so far termed 'bacterial' (subclass Ic and III) or 'fungal' (subclass II and V) [14,17]. This wide distribution is reminiscent of the diverse evolutionary pathways of algae [e.g. [51]]. The unicellular green alga *C. reinhardtii* shares many genes with both animals [52] and bacteria [e.g. [53]], and this genetic mosaic is reflected in the phylogenetics of its four OYE proteins, which are grouped into three different OYE subclasses. The characterization of recombinant forms of CrOYE1-3, representatives of three evolutionary distinct groups, revealed that these enzymes are functional OYEs exhibiting different biochemical properties, which might be exploited for targeted applications, including whole-cell biotransformation processes employing the natural host, *C. reinhardtii*.

4.2. The three phylogenetically distinct OYEs from C. reinhardtii exhibit biochemical variance

The recombinant forms of *C. reinhardtii* CrOYE1-3 are functional OYEs as shown by their tight binding of FMN (Fig. S1, Supporting Information) and their capability to catalyze the NADPH-dependent reduction of a broad spectrum of known OYE substrates (Table 1). Notable characteristics of the green algal enzymes are (a) the similar substrate scope of CrOYE1 and CrOYE2 despite their primary sequence-based classification in different phylogenetic groups, (b) the unusually narrow substrate scope of CrOYE3, an evolutionary outlier, and (c) the variable sensitivity towards inhibition by NMI.

CrOYE1 and CrOYE2 were found to catalyze the reduction of a very similar substrate range (Table 1), which is similar to that of the model bacterial ene reductase YqjM [38,54]. Notably, while CrOYE1, as YqjM, was phylogenetically grouped with subclass III OYEs, CrOYE2 belongs to subclass Ib (Fig. 2). An analysis of subclass I *versus* III OYE members has indicated different biochemical properties and substrate preferences [14], which CrOYE1 and CrOYE2 do not follow. This suggests that phylogenetically close OYEs, due to varying habitat requirements of their hosts, might have evolved specialized structure-function relationships, which need to be elucidated yet.

Regarding economic applicability, both CrOYE1 and CrOYE2 have a conversion efficiency on several substrates of industrial interest similar to or better than known OYEs, suggesting that they might be useful for industrial processes either as free enzymes or within living algal cells (also see below). CrOYE2, for example, converts ketoisophorone (KIP) faster than the *Synechococcus* OYE SynER [55]. KIP is an important intermediate for the production of carotenoids, such as zeaxanthin and xanthoxin [56]. Both CrOYE1 and CrOYE2 reduce carvones as fast as OYEs that were previously reported to exhibit high velocities, namely

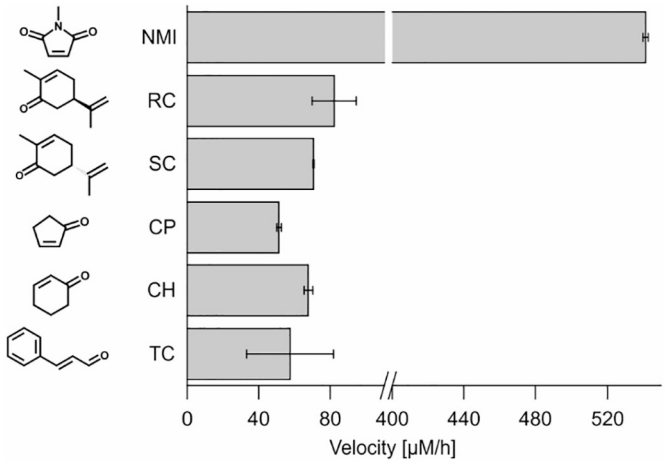

Fig. 4. Conversion rates of OYE model substrates by *C. reinhardtii* cultures. Strain CC-5325 was grown to the exponential phase and then concentrated to 100 μg Chl × mL^{-1}. The cells were incubated in the presence of 1 mM substrate in the light. Conversion velocities were determined in the linear range of substrate consumption (see Fig. S4, Supporting Information). The experiments were biologically repeated at least twice. Columns show the mean values, error bars the standard deviation.

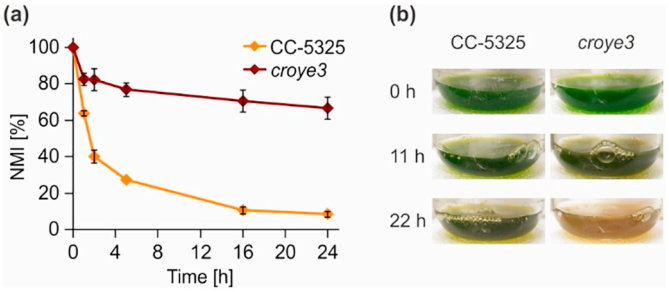

Fig. 5. *In vivo* conversion of NMI by the *C. reinhardtii* wild type CC-5325 and by the *croye3* mutant. Exponentially growing algal cells were concentrated to 100 μg Chl × mL^{-1} and incubated with 1 mM substrate. (a): Residual NMI was quantified at defined time points. The experiments were done in triplicate. Data points show the mean values, error bars indicate the standard deviation. (b): The appearance of the cells was documented photographically after 0 h, 11 h and 22 h of the biotransformation experiment.

YersER from the bacterium *Yersinia bercovieri* [57], ClER from the yeast *Clavispora lusitaniae* [58] or *Bacillus* Bac-OYE1 [59]. Dihydrocarvones are applied as inhibitors of bacteria and fungi and as insect repellents [[60], and references therein]. Additionally, they are valuable precursors for pharmaceutically relevant compounds such as antimalarial drugs [61] and other chiral and natural products [62–64].

CrOYE3 was identified as a phylogenetic outlier close to both subclass I and subclass II enzymes (Fig. 2). From the substrates tested here, it only converted maleimides (Table 1). To our knowledge, all previously in-depth characterized OYEs have a broader scope and usually significantly lower specific activities for maleimides. This might indicate that there is still a substrate group of unrelated structural characteristics that was not investigated yet and may be closer to the true physiological substrates. Broadening the *in vitro* substrate scope is thus required in the future. Besides the preference for maleimides, CrOYE3 exhibits a very high activity on NMI (Table 1). Although OYEs with high NMI conversion activities have been reported before [18,57,65–67], CrOYE3 is outstanding among the wild type forms of previously analyzed OYEs. Interestingly, a putative OYE (VcOYE1) from *Volvox carteri*, a close relative of *C. reinhardtii*, but multicellular [68], shows a very high sequence conservation to CrOYE3. The investigation of these sequentially similar enzymes may shed light on the unique properties of CrOYE3 and CrOYE3-like enzymes, respectively.

Maleimides, despite being efficiently converted substrates, inactivate certain subclasses of OYEs over time. In OYERo2a from *R. opacus*, Cys25, which is conserved in subclass III OYEs and proposed to influence the FMN redox potential [69], is responsible for the irreversibly inhibiting effect [50]. Having at hand OYE representatives from different phylogenetic subclasses, we investigated the effect of NMI on CrOYE1–3. In case of CrOYE1 and YqjM, grouped in subclass III and featuring the conserved cysteine residue (Fig. 3b), the expected inhibitory effect of NMI was indeed observed. An exchange of this residue in CrOYE1 to serine prevented NMI-dependent inactivation and increased the reaction rate (Fig. 3a), similar to previous results on OYERo2a [50], supporting the role of this position. CrOYE2 and CrOYE3 feature a threonine instead of a cysteine at the position that is attacked by NMI in OYERo2a and CrOYE1. CrOYE2 met our hypothesis that this would protect the enzymes from inhibition by NMI, however, CrOYE3 was inhibited by NMI. All three *C. reinhardtii* OYEs contain several mostly non-conserved cysteine residues (CrOYE1: six, CrOYE2: five, CrOYE3: four), suggesting that NMI attacks one of these cysteines in CrOYE3. As cysteines very often play important roles in enzymes, be it as catalytic modulators or by providing means for disulfide bridges and redox regulation, investigating the role the additional cysteines in the algal OYEs appears a promising strategy to dig deeper into the structure-function relationships of OYEs.

4.3. Algal whole-cell biocatalysis complements CrOYE in vitro characterization

Microbial fermentation products are already firmly established in our industries. In living cells, enzymes work in their naturally optimized environments and are permanently regenerated by the cells' anabolic processes. In case of enzymes requiring co-substrates such as NAD(P)H, the metabolic recycling of this commercially costly substance is an additional advantage. The employment of organisms that carry out oxygenic photosynthesis is regarded as promising for future climate-friendly sustainable processes [e.g. [70]]. Although many hurdles are yet to take, such as an efficient provision of light and carbon dioxide, the light-dependent regeneration of NADPH is a huge advantage over heterotrophic processes that require bio-accessible carbon sources. Kourist and coworkers developed the cyanobacterium *Synechocystis* sp. as a whole-cell biocatalyst for different enzyme classes [27,71]. Recombinant cyanobacterial cells expressing the ene reductase YqjM were indeed able to convert model substrates with a rate comparable to *E. coli* or yeast.

Here, we show that the unicellular green alga *C. reinhardtii* is also suited for cellular ene reduction (Fig. 4; Fig. S4, Supporting Information). Methodically, we developed an easy and robust extraction procedure suitable for the quantification of whole-cell algal biocatalysis samples based on ethyl acetate, which was sufficient for the extraction of our target compounds. The substrates we tested were converted to the expected products by wild type cultures. The absence of product formation in cell-free supernatants indicates that the substrates were taken up and most likely converted intracellularly, possibly in the chloroplast, as all four OYEs from *C. reinhardtii* are predicted to possess N-terminal chloroplast targeting sequences.

Cellular conversion rates reached 0.54 mM × h^{-1} in case of NMI as a substrate, which lies in the same order of magnitude as observed for a cyanobacterial whole-cell system developed by Büchsenschütz et al., 2019 [72] who employed recombinant cells. The fact that wild type *C. reinhardtii* cells are already reasonably efficient bears huge potential for further optimization, for example through homologous or heterologous overexpression of ene reductase sequences. Overexpression of OYE-encoding sequences in the chloroplast, the compartment of photosynthetic NADPH generation, appears particularly promising and has

been shown before to work well for both heterologous [e.g. [73]] and homologous genes [e.g. [74]]. Algal-based whole-cell biotransformation systems might thus represent alternatives to the attempts of optimizing OYEs to accept cheaper nicotinamide co-substrates and chemical mimics [15,70,75–77].

Notably, *C. reinhardtii* whole-cell substrate conversion rates mirrored *in vitro* enzymatic activities with regard to the very high NMI reduction rate (Fig. 4). In accordance with the high *in vitro* activity of CrOYE3, compared to the rates observed for CrOYE1 and CrOYE2, NMI was hardly converted in a *C. reinhardtii croye3* mutant strain, suggesting that CrOYE3 is the most active NMI-reducing enzyme also intracellularly.

The physiological function of ene reductases in *C. reinhardtii* remains to be elucidated. Despite intense investigation and application of various ene reductases from diverse origins in research and industry, the physiological role and natural substrates of this enzyme class remain mostly unknown. One assumption is that OYEs are involved in the oxidative stress response [38,78,79]. OYEs have also been implicated in detoxifying environmental compounds [80–82]. In plants, 12-oxophytodienoate reductases (OPRs) are members of the OYE family and participate in octadecanoid synthesis by reduction of 12-oxophytodienoic acid to 12-oxo phytoenoic acid within the jasmonic acid synthesis pathway [83,84]. Not much information is available on the effects of phytohormones in *C. reinhardtii*, however, some phytohormones show an effect [85,86], and biosynthetic pathways for jasmonate and other phytohormones have been predicted to be present in the alga [86–88]. Still, as OYEs are very promiscuous *in vitro*, identifying the natural substrates of the CrOYEs will be difficult to tackle. The availability of mutants, combined with metabolomics approaches might shed light on this biological question.

5. Conclusion

Carbon-carbon double bond reductases are important biocatalysts for the stereoselective hydrogenation of activated alkenes. Here, we complement previously annotated OYE subclasses by putative OYE sequences from eukaryotic, photosynthetically active organisms. Three OYEs from *C. reinhardtii* belonging to different phylogenetic subclasses show distinct features regarding their substrate scope and the mode-of-action of the OYE inhibitor NMI. The narrow substrate scope of CrOYE3 is surprising and promises new insights into structure-function-relationships of OYEs. Whole-cell ene reduction by *C. reinhardtii* is feasible and reasonably efficient even in wild type cells, providing much room for metabolic engineering or synthetic biology optimization strategies.

CRediT authorship contribution statement

Stefanie Böhmer:Methodology, Investigation, Validation, Writing - original draft, Visualization.**Christina Marx**:Conceptualization, Methodology, Validation, Writing - original draft, Visualization, Supervision.**Álvaro Gómez-Baraibar**:Methodology, Investigation, Validation.**Marc M. Nowaczyk**:Methodology, Investigation, Validation, Resources, Funding acquisition.**Dirk Tischler**:Methodology, Investigation, Validation, Funding acquisition.**Anja Hemschemeier**:Conceptualization, Methodology, Validation, Writing - review & editing, Supervision, Funding acquisition.**Thomas Happe**:Conceptualization, Validation, Resources, Writing - review & editing, Supervision, Project administration, Funding acquisition.

Declaration of competing interest

The authors declare that they have no known competing financial interests or personal relationships that could have appeared to influence the work reported in this paper.

Acknowledgements

We thank the Deutsche Forschungsgemeinschaft for funding (RTG 2341 MiCon to M.N., D.T., A.H. and T.H.) D.T. was also supported by the Federal Ministry for Innovation, Science and Research of North Rhine-Westphalia (PtJ-TRI/1411ng006)-ChemBioCat. S.B. acknowledges a PhD scholarship from the Studienstiftung des deutschen Volkes. We also thank Hetti Bregulla for excellent experimental support.

Appendix A. Supplementary data

Supplementary data to this article can be found online at https://doi.org/10.1016/j.algal.2020.101970.

References

[1] J.A. Littlechild, Improving the 'tool box' for robust industrial enzymes, J. Ind. Microbiol. Biotechnol. 44 (2017) 711–720, https://doi.org/10.1007/s10295-017-1920-5.
[2] S. Serra, C. Fuganti, E. Brenna, Biocatalytic preparation of natural flavours and fragrances, Trends Biotechnol. 23 (2005) 193–198, https://doi.org/10.1016/j.tibtech.2005.02.003.
[3] B. Lin, Y. Tao, Whole-cell biocatalysts by design, Microb. Cell Factories 16 (2017) 106, https://doi.org/10.1186/s12934-017-0724-7.
[4] G. Zassinovich, G. Mestroni, S. Gladiali, Asymmetric hydrogen transfer reactions promoted by homogeneous transition metal catalysts, Chem. Rev. 92 (1992) 1051–1069, https://doi.org/10.1021/cr00013a015.
[5] A. Dhakshinamoorthy, M. Alvaro, H. Garcia, Metal-organic frameworks (MOFs) as heterogeneous catalysts for the chemoselective reduction of carbon-carbon multiple bonds with hydrazine, Adv. Synth. Catal. 351 (2009) 2271–2276, https://doi.org/10.1002/adsc.200900362.
[6] E.J. Lenardão, G.V. Botteselle, F. de Azambuja, G. Perin, R.G. Jacob, Citronellal as key compound in organic synthesis, Tetrahedron 63 (2007) 6671–6712, https://doi.org/10.1016/j.tet.2007.03.159.
[7] K. Tani, T. Yamagata, S. Akutagawa, H. Kumobayashi, T. Taketomi, H. Takaya, A. Miyashita, R. Noyori, S. Otsuka, Metal-assisted terpenoid synthesis. 7. Highly enantioselective isomerization of prochiral allylamines catalyzed by chiral diphosphine rhodium(I) complexes. Preparation of optically active enamines, J. Am. Chem. Soc. 106 (1984) 5208–5217, https://doi.org/10.1021/ja00330a029.
[8] S. Akutagawa, Enantioselective isomerization of allylamine to enamine: practical asymmetric synthesis of (–)-menthol by Rh–BINAP catalysts, Top. Catal. 4 (1997) 271–274, https://doi.org/10.1023/A:1019112911246.
[9] L. Zheng, J. Lin, B. Zhang, Y. Kuang, D. Wei, Identification of a yeast old yellow enzyme for highly enantioselective reduction of citral isomers to (*R*)-citronellal, Bioresources and Bioprocessing 5 (2018) 9, https://doi.org/10.1186/s40643-018-0192-x.
[10] R. Stürmer, B. Hauer, M. Hall, K. Faber, Asymmetric bioreduction of activated C=C bonds using enoate reductases from the old yellow enzyme family, Curr. Opin. Chem. Biol. 11 (2007) 203–213, https://doi.org/10.1016/j.cbpa.2007.02.025.
[11] C. Breithaupt, J. Strassner, U. Breitinger, R. Huber, P. Macheroux, A. Schaller, T. Clausen, X-ray structure of 12-oxophytodienoate reductase 1 provides structural insight into substrate binding and specificity within the family of OYE, Structure 9 (2001) 419–429, https://doi.org/10.1016/s0969-2126(01)00602-5.
[12] H.S. Toogood, J.M. Gardiner, N.S. Scrutton, Biocatalytic reductions and chemical versatility of the old yellow enzyme family of flavoprotein oxidoreductases, ChemCatChem 2 (2010) 892–914, https://doi.org/10.1002/cctc.201000094.
[13] F. Luo, D. Lu, Y. Gong, Enantioselective bioreduction of 2-fluoro-2-alken-1-ols mediated by *Saccharomyces cerevisiae*, J. Mol. Catal. B Enzym. 70 (2011) 101–107, https://doi.org/10.1016/j.molcatb.2011.02.011.
[14] A. Scholtissek, D. Tischler, A.H. Westphal, W.J.H. Van Berkel, C.E. Paul, Old yellow enzyme-catalysed asymmetric hydrogenation: linking family roots with improved catalysis, Catalysts 7 (2017) 130, https://doi.org/10.3390/catal7050130.
[15] C.E. Paul, S. Gargiulo, D.J. Opperman, I. Lavandera, V. Gotor-Fernández, V. Gotor, A. Taglieber, I.W. Arends, F. Hollmann, Mimicking nature: synthetic nicotinamide cofactors for C=C bioreduction using enoate reductases, Org. Lett. 15 (2013) 180–183, https://doi.org/10.1021/ol303240a.
[16] O. Warburg, W. Christian, Ein zweites sauerstoffübertragendes Ferment und sein Absorptionsspektrum, Naturwissenschaften 20 (1932) 688, https://doi.org/10.1007/bf01494406.
[17] C. Peters, D. Frasson, M. Sievers, R. Buller, Novel old yellow enzyme subclasses, ChemBioChem 20 (2019) 1569–1577, https://doi.org/10.1002/cbic.201800770.
[18] A. Scholtissek, S.R. Ullrich, M. Mühling, M. Schlömann, C.E. Paul, D. Tischler, A thermophilic-like ene-reductase originating from an acidophilic iron oxidizer, Appl. Microbiol. Biotechnol. 101 (2017) 609–619, https://doi.org/10.1007/s00253-016-7782-3.
[19] G. Steinkellner, C.C. Gruber, T. Pavkov-Keller, A. Binter, K. Steiner, C. Winkler, A. Łyskowski, O. Schwamberger, M. Oberer, H. Schwab, K. Faber, P. Macheroux, K. Gruber, Identification of promiscuous ene-reductase activity by mining structural databases using active site constellations, Nat. Commun. 5 (2014) 4150, https://doi.org/10.1038/ncomms5150.
[20] E.D. Amato, J.D. Stewart, Applications of protein engineering to members of the old

yellow enzyme family, Biotechnol. Adv. 33 (2015) 624–631, https://doi.org/10.1016/j.biotechadv.2015.04.011.
[21] M. Crotti, F. Parmeggiani, E.E. Ferrandi, F.G. Gatti, A. Sacchetti, S. Riva, E. Brenna, D. Monti, Stereoselectivity switch in the reduction of α-alkyl-β-arylenones by structure-guided designed variants of the ene reductase OYE1, Frontiers in Bioengineering and Biotechnology 7 (2019), https://doi.org/10.3389/fbioe.2019.00089.
[22] X. Ying, S. Yu, M. Huang, R. Wei, S. Meng, F. Cheng, M. Yu, M. Ying, M. Zhao, Z. Wang, Engineering the enantioselectivity of yeast old yellow enzyme OYE2y in asymmetric reduction of (*E/Z*)-Citral to (*R*)-citronellal, Molecules 24 (2019), https://doi.org/10.3390/molecules24061057.
[23] M.S. Robescu, M. Niero, M. Hall, L. Cendron, E. Bergantino, Two new ene-reductases from photosynthetic extremophiles enlarge the panel of old yellow enzymes: *Ct*OYE and *Gs*OYE, Appl. Microbiol. Biotechnol. 104 (2020) 2051–2066, https://doi.org/10.1007/s00253-019-10287-2.
[24] K. Dumorné, D.C. Córdova, M. Astorga-Eló, P. Renganathan, Extremozymes: a potential source for industrial applications, J. Microbiol. Biotechnol. 27 (2017) 649–659, https://doi.org/10.4014/jmb.1611.11006.
[25] D. Tischler, E. Gädke, D. Eggerichs, A. Gomez Baraibar, C. Mügge, A. Scholtissek, C.E. Paul, Asymmetric reduction of (*R*)-carvone through a thermostable and organic-solvent-tolerant ene-reductase, ChemBioChem (2020), https://doi.org/10.1002/cbic.201900599 Epub ahead of print.
[26] K. Castiglione, Y. Fu, I. Polte, S. Leupold, A. Meo, D. Weuster-Botz, Asymmetric whole-cell bioreduction of (*R*)-carvone by recombinant *Escherichia coli* with *in situ* substrate supply and product removal, Biochem. Eng. J. 117 (2017) 102–111, https://doi.org/10.1016/j.bej.2016.10.002.
[27] K. Köninger, A. Gómez Baraibar, C. Mügge, C.E. Paul, F. Hollmann, M.M. Nowaczyk, R. Kourist, Recombinant cyanobacteria for the asymmetric reduction of C=C bonds fueled by the biocatalytic oxidation of water, Angew Chem Int Ed Engl 55 (2016) 5582–5585, https://doi.org/10.1002/anie.201601200.
[28] X. Li, W. Patena, F. Fauser, R.E. Jinkerson, S. Saroussi, M.T. Meyer, N. Ivanova, J.M. Robertson, R. Yue, R. Zhang, J. Vilarrasa-Blasi, T.M. Wittkopp, S. Ramundo, S.R. Blum, A. Goh, M. Laudon, T. Srikumar, P.A. Lefebvre, A.R. Grossman, M.C. Jonikas, A genome-wide algal mutant library and functional screen identifies genes required for eukaryotic photosynthesis, Nat. Genet. 51 (2019) 627–635, https://doi.org/10.1038/s41588-019-0370-6.
[29] E.H. Harris, The *Chlamydomonas* Sourcebook: A Comprehensive Guide to Biology and Laboratory Use, Academic Press, San Diego, 1989, https://doi.org/10.1016/C2009-0-02778-0.
[30] S.M. Newman, J.E. Boynton, N.W. Gillham, B.L. Randolph-Anderson, A.M. Johnson, E.H. Harris, Transformation of chloroplast ribosomal RNA genes in *Chlamydomonas*: molecular and genetic characterization of integration events, Genetics 126 (1990) 875–888.
[31] D. Simon, S. Helliwell, Extraction and quantification of chlorophyll *a* from freshwater green algae, Water Res. 32 (1998) 2220–2223, https://doi.org/10.1016/S0043-1354(97)00452-1.
[32] A. Hemschemeier, D. Casero, B. Liu, C. Benning, M. Pellegrini, T. Happe, S.S. Merchant, Copper response regulator1-dependent and -independent responses of the *Chlamydomonas reinhardtii* transcriptome to dark anoxia, Plant Cell 25 (2013) 3186–3211, https://doi.org/10.1105/tpc.113.115741.
[33] H. Liu, J.H. Naismith, An efficient one-step site-directed deletion, insertion, single and multiple-site plasmid mutagenesis protocol, BMC Biotechnol. 8 (2008) 91, https://doi.org/10.1186/1472-6750-8-91.
[34] E.S. Lennox, Transduction of linked genetic characters of the host by bacteriophage P1, Virology 1 (1955) 190–206, https://doi.org/10.1016/0042-6822(55)90016-7.
[35] A. Riedel, M. Mehnert, C.E. Paul, A.H. Westphal, W.J. van Berkel, D. Tischler, Functional characterization and stability improvement of a 'thermophilic-like' ene-reductase from *Rhodococcus opacus* 1CP, Front. Microbiol. 6 (2015) 1073, https://doi.org/10.3389/fmicb.2015.01073.
[36] S. Wang, H. Huang, J. Moll, R.K. Thauer, $NADP^+$ reduction with reduced ferredoxin and $NADP^+$ reduction with NADH are coupled via an electron-bifurcating enzyme complex in *Clostridium kluyveri*, J. Bacteriol. 192 (2010) 5115–5123, https://doi.org/10.1128/JB.00612-10.
[37] H.T.S. Britton, R.A. Robinson, CXCVIII.—universal buffer solutions and the dissociation constant of veronal, Journal of the Chemical Society (Resumed) (1931) 1456–1462, https://doi.org/10.1039/JR9310001456.
[38] T.B. Fitzpatrick, N. Amrhein, P. Macheroux, Characterization of YqjM, an old yellow enzyme homolog from *Bacillus subtilis* involved in the oxidative stress response, J. Biol. Chem. 278 (2003) 19891–19897, https://doi.org/10.1074/jbc.M211778200.
[39] M. Hall, C. Stueckler, W. Kroutil, P. Macheroux, K. Faber, Asymmetric bioreduction of activated alkenes using cloned 12-oxophytodienoate reductase isoenzymes OPR-1 and OPR-3 from *Lycopersicon esculentum* (tomato): a striking change of stereoselectivity, Angew Chem Int Ed Engl 46 (2007) 3934–3937, https://doi.org/10.1002/anie.200605168.
[40] S.F. Altschul, W. Gish, W. Miller, E.W. Myers, D.J. Lipman, Basic local alignment search tool, J. Mol. Biol. 215 (1990) 403–410, https://doi.org/10.1016/S0022-2836(05)80360-2.
[41] J.D. Thompson, D.G. Higgins, T.J. Gibson, CLUSTAL W: improving the sensitivity of progressive multiple sequence alignment through sequence weighting, position-specific gap penalties and weight matrix choice, Nucleic Acids Res. 22 (1994) 4673–4680, https://doi.org/10.1093/nar/22.22.4673.
[42] D.T. Jones, W.R. Taylor, J.M. Thornton, The rapid generation of mutation data matrices from protein sequences, Comput. Appl. Biosci. 8 (1992) 275–282, https://doi.org/10.1093/bioinformatics/8.3.275.
[43] S. Kumar, G. Stecher, K. Tamura, MEGA7: molecular evolutionary genetics analysis version 7.0 for bigger datasets, Mol. Biol. Evol. 33 (2016) 1870–1874, https://doi.org/10.1093/molbev/msw054.
[44] S. Nizam, S. Verma, N.N. Borah, R.K. Gazara, P.K. Verma, Comprehensive genome-wide analysis reveals different classes of enigmatic old yellow enzyme in fungi, Sci. Rep. 4 (2014) 4013, https://doi.org/10.1038/srep04013.
[45] K. Kitzing, T.B. Fitzpatrick, C. Wilken, J. Sawa, G.P. Bourenkov, P. Macheroux, T. Clausen, The 1.3 Å crystal structure of the flavoprotein YqjM reveals a novel class of old yellow enzymes, J. Biol. Chem. 280 (2005) 27904–27913, https://doi.org/10.1074/jbc.M502587200.
[46] S.D. Gallaher, S.T. Fitz-Gibbon, A.G. Glaesener, M. Pellegrini, S.S. Merchant, *Chlamydomonas* genome resource for laboratory strains reveals a mosaic of sequence variation, identifies true strain histories, and enables strain-specific studies, Plant Cell 27 (2015) 2335–2352, https://doi.org/10.1105/tpc.15.00508.
[47] P. Horton, K.-J. Park, T. Obayashi, N. Fujita, H. Harada, C.J. Adams-Collier, K. Nakai, WoLF PSORT: protein localization predictor, Nucleic Acids Res. 35 (2007) W585–W587, https://doi.org/10.1093/nar/gkm259.
[48] M. Tardif, A. Atteia, M. Specht, G. Cogne, N. Rolland, S. Brugière, M. Hippler, M. Ferro, C. Bruley, G. Peltier, O. Vallon, L. Cournac, PredAlgo: a new subcellular localization prediction tool dedicated to green algae, Mol. Biol. Evol. 29 (2012) 3625–3639, https://doi.org/10.1093/molbev/mss178.
[49] O. Emanuelsson, H. Nielsen, G.V. Heijne, ChloroP, a neural network-based method for predicting chloroplast transit peptides and their cleavage sites, Protein Sci. 8 (1999) 978–984, https://doi.org/10.1110/ps.8.5.978.
[50] A. Scholtissek, E. Gadke, C.E. Paul, A.H. Westphal, W.J.H. van Berkel, D. Tischler, Catalytic performance of a class III old yellow enzyme and its cysteine variants, Front. Microbiol. 9 (2018) 2410, https://doi.org/10.3389/fmicb.2018.02410.
[51] L. Tirichine, C. Bowler, Decoding algal genomes: tracing back the history of photosynthetic life on Earth, Plant J. 66 (2011) 45–57, https://doi.org/10.1111/j.1365-313X.2011.04540.x.
[52] S.S. Merchant, S.E. Prochnik, O. Vallon, E.H. Harris, S.J. Karpowicz, G.B. Witman, A. Terry, A. Salamov, L.K. Fritz-Laylin, L. Maréchal-Drouard, W.F. Marshall, L.H. Qu, D.R. Nelson, A.A. Sanderfoot, M.H. Spalding, V.V. Kapitonov, Q. Ren, P. Ferris, E. Lindquist, H. Shapiro, S.M. Lucas, J. Grimwood, J. Schmutz, P. Cardol, H. Cerutti, G. Chanfreau, C.L. Chen, V. Cognat, M.T. Croft, R. Dent, S. Dutcher, E. Fernández, H. Fukuzawa, D. González-Ballester, D. González-Halphen, A. Hallmann, M. Hanikenne, M. Hippler, W. Inwood, K. Jabbari, M. Kalanon, R. Kuras, P.A. Lefebvre, S.D. Lemaire, A.V. Lobanov, M. Lohr, A. Manuell, I. Meier, L. Mets, M. Mittag, T. Mittelmeier, J.V. Moroney, J. Moseley, C. Napoli, A.M. Nedelcu, K. Niyogi, S.V. Novoselov, I.T. Paulsen, G. Pazour, S. Purton, J.P. Ral, D.M. Riano-Pachón, W. Riekhof, L. Rymarquis, M. Schroda, D. Stern, J. Umen, R. Willows, N. Wilson, S.L. Zimmer, J. Allmer, J. Balk, K. Bisova, C.J. Chen, M. Elias, K. Gendler, C. Hauser, M.R. Lamb, H. Ledford, J.C. Long, J. Minagawa, M.D. Page, J. Pan, W. Pootakham, S. Roje, A. Rose, E. Stahlberg, A.M. Terauchi, P. Yang, S. Ball, C. Bowler, C.L. Dieckmann, V.N. Gladyshev, P. Green, R. Jorgensen, S. Mayfield, B. Mueller-Roeber, S. Rajamani, R.T. Sayre, P. Brokstein, I. Dubchak, D. Goodstein, L. Hornick, Y.W. Huang, J. Jhaveri, Y. Luo, D. Martinez, W.C. Ngau, B. Otillar, A. Poliakov, A. Porter, L. Szajkowski, G. Werner, K. Zhou, I.V. Grigoriev, D.S. Rokhsar, A.R. Grossman, The *Chlamydomonas* genome reveals the evolution of key animal and plant functions, Science 318 (2007) 245–250, https://doi.org/10.1126/science.1143609.
[53] A. Hemschemeier, Chlamydomonas: Anoxic acclimation and signaling, in: M. Hippler (Ed.), Chlamydomonas: Molecular Genetics and Physiology, Springer International Publishing, Cham, 2017, pp. 155–199, , https://doi.org/10.1007/978-3-319-66365-4_6.
[54] M. Pesic, E. Fernández-Fueyo, F. Hollmann, Characterization of the old yellow enzyme homolog from *Bacillus subtilis* (YqjM), ChemistrySelect 2 (2017) 3866–3871, https://doi.org/10.1002/slct.201700724.
[55] Y. Fu, K. Hoelsch, D. Weuster-Botz, A novel ene-reductase from *Synechococcus* sp. PCC 7942 for the asymmetric reduction of alkenes, Process Biochem. 47 (2012) 1988–1997, https://doi.org/10.1016/j.procbio.2012.07.009.
[56] H.G.W. Leuenberger, W. Boguth, E. Widmer, R. Zell, Synthese von optisch aktiven, natürlichen Carotinoiden und strukturell verwandten Naturprodukten. I. Synthese der chiralen Schlüsselverbindung (4R, 6R)-4-Hydroxy-2,2,6-trimethylcyclohexanon, Helv. Chim. Acta 59 (1976) 1832–1849, https://doi.org/10.1002/hlca.19760590541.
[57] J.F. Chaparro-Riggers, T.A. Rogers, E. Vazquez-Figueroa, K.M. Polizzi, A.S. Bommarius, Comparison of three enoate reductases and their potential use for biotransformations, Adv. Synth. Catal. 349 (2007) 1521–1531, https://doi.org/10.1002/adsc.200700074.
[58] Y. Ni, H.-L. Yu, G.-Q. Lin, J.-H. Xu, An ene reductase from *Clavispora lusitaniae* for asymmetric reduction of activated alkenes, Enzym. Microb. Technol. 56 (2014) 40–45, https://doi.org/10.1016/j.enzmictec.2013.12.016.
[59] H. Zhang, X. Gao, J. Ren, J. Feng, T. Zhang, Q. Wu, D. Zhu, Enzymatic hydrogenation of diverse activated alkenes. Identification of two *Bacillus* old yellow enzymes with broad substrate profiles, J. Mol. Catal. B Enzym. 105 (2014) 118–125, https://doi.org/10.1016/j.molcatb.2014.04.004.
[60] C. Porto, C.Z. Stüker, A.S. Mallmann, E. Simionatto, A. Flach, T.d. Canto-Dorow, U.F.d. Silva, I.I. Dalcol, A.F. Morel, (*R*)-(-)-carvone and (1*R*, 4*R*)-*trans*-(+)-dihydrocarvone from *Poiretia latifolia* vogel, J. Braz. Chem. Soc. 21 (2010) 782–786, https://doi.org/10.1590/S0103-50532010000500003.
[61] Y. Dong, K.J. McCullough, S. Wittlin, J. Chollet, J.L. Vennerstrom, The structure and antimalarial activity of dispiro-1,2,4,5-tetraoxanes derived from (+)-dihydrocarvone, Bioorg. Med. Chem. Lett. 20 (2010) 6359–6361, https://doi.org/10.1016/j.bmcl.2010.09.113.
[62] D.C. Harrowven, D.D. Pascoe, D. Demurtas, H.O. Bourne, Total synthesis of (−)-Colombiasin a and (−)-Elisapterosin B, Angew. Chem. Int. Ed. 44 (2005)

1221–1222, https://doi.org/10.1002/anie.200462268.
[63] Y. Aubin, G. Audran, H. Monti, Improved enantioselective synthesis of natural striatenic acid and its methyl ester, Tetrahedron Lett. 47 (2006) 3669–3671, https://doi.org/10.1016/j.tetlet.2006.03.147.
[64] G. Blay, B. Garcia, E. Molina, J.R. Pedro, Synthesis of (+)-pechueloic acid and (+)-aciphyllene. Revision of the structure of (+)-aciphyllene, Tetrahedron 63 (2007) 9621–9626, https://doi.org/10.1016/j.tet.2007.07.039.
[65] M.-Y. Xu, X.-Q. Pei, Z.-L. Wu, Identification and characterization of a novel "thermophilic-like" Old Yellow Enzyme from the genome of *Chryseobacterium* sp. CA49, J. Mol. Catal. B Enzym. 108 (2014) 64–71, https://doi.org/10.1016/j.molcatb.2014.07.002.
[66] Y. Fu, K. Castiglione, D. Weuster-Botz, Comparative characterization of novel ene-reductases from cyanobacteria, Biotechnol. Bioeng. 110 (2013) 1293–1301, https://doi.org/10.1002/bit.24817.
[67] B.V. Adalbjörnsson, H.S. Toogood, A. Fryszkowska, C.R. Pudney, T.A. Jowitt, D. Leys, N.S. Scrutton, Biocatalysis with thermostable enzymes: structure and properties of a thermophilic 'ene'-reductase related to old yellow enzyme, ChemBioChem 11 (2010) 197–207, https://doi.org/10.1002/cbic.200900570.
[68] S.E. Prochnik, J. Umen, A.M. Nedelcu, A. Hallmann, S.M. Miller, I. Nishii, P. Ferris, A. Kuo, T. Mitros, L.K. Fritz-Laylin, U. Hellsten, J. Chapman, O. Simakov, S.A. Rensing, A. Terry, J. Pangilinan, V. Kapitonov, J. Jurka, A. Salamov, H. Shapiro, J. Schmutz, J. Grimwood, E. Lindquist, S. Lucas, I.V. Grigoriev, R. Schmitt, D. Kirk, D.S. Rokhsar, Genomic analysis of organismal complexity in the multicellular green alga *Volvox carteri*, Science 329 (2010) 223–226, https://doi.org/10.1126/science.1188800.
[69] O. Spiegelhauer, S. Mende, F. Dickert, S.H. Knauer, G.M. Ullmann, H. Dobbek, Cysteine as a modulator residue in the active site of xenobiotic reductase A: a structural, thermodynamic and kinetic study, J. Mol. Biol. 398 (2010) 66–82, https://doi.org/10.1016/j.jmb.2010.02.044.
[70] R.H. Wijffels, O. Kruse, K.J. Hellingwerf, Potential of industrial biotechnology with cyanobacteria and eukaryotic microalgae, Curr. Opin. Biotechnol. 24 (2013) 405–413, https://doi.org/10.1016/j.copbio.2013.04.004.
[71] S. Böhmer, K. Köninger, Á. Gómez-Baraibar, S. Bojarra, C. Mügge, S. Schmidt, M.M. Nowaczyk, R. Kourist, Enzymatic Oxyfunctionalization driven by photosynthetic water-splitting in the cyanobacterium *Synechocystis* sp. PCC 6803, Catalysts 7 (2017) 240, https://doi.org/10.3390/catal7080240.
[72] H.C. Büchsenschütz, V. Vidimce-Risteski, B. Eggbauer, S. Schmidt, C.K. Winkler, J.H. Schrittwieser, W. Kroutil, R. Kourist, Stereoselective biotransformations of cyclic imines in recombinant cells of *Synechocystis* sp. PCC 6803, ChemCatChem 12 (2019) 726–730, https://doi.org/10.1002/cctc.201901592.
[73] Y.M. Dyo, S. Purton, The algal chloroplast as a synthetic biology platform for production of therapeutic proteins, Microbiology 164 (2018) 113–121, https://doi.org/10.1099/mic.0.000599.
[74] A. Sawyer, Y. Bai, Y. Lu, A. Hemschemeier, T. Happe, Compartmentalisation of [FeFe]-hydrogenase maturation in *Chlamydomonas reinhardtii*, Plant J. 90 (2017) 1134–1143, https://doi.org/10.1111/tpj.13535.
[75] C. Mähler, F. Kratzl, M. Vogel, S. Vinnenberg, D. Weuster-Botz, K. Castiglione, Loop swapping as a potent approach to increase ene reductase activity with nicotinamide adenine dinucleotide (NADH), Adv. Synth. Catal. 361 (2019) 2505–2513, https://doi.org/10.1002/adsc.201900073.
[76] A.I. Iorgu, T.M. Hedison, S. Hay, N.S. Scrutton, Selectivity through discriminatory induced fit enables switching of NAD(P)H coenzyme specificity in Old Yellow Enzyme ene-reductases, FEBS J. 286 (2019) 3117–3128, https://doi.org/10.1111/febs.14862.
[77] C.J. Seel, T. Gulder, Biocatalysis fueled by light: on the versatile combination of photocatalysis and enzymes, ChemBioChem 20 (2019) 1871–1897, https://doi.org/10.1002/cbic.201800806.
[78] S. Ehira, H. Teramoto, M. Inui, H. Yukawa, A novel redox-sensing transcriptional regulator CyeR controls expression of an Old Yellow Enzyme family protein in *Corynebacterium glutamicum*, Microbiology 156 (2010) 1335–1341, https://doi.org/10.1099/mic.0.036913-0.
[79] T.R. Hurd, T.A. Prime, M.E. Harbour, K.S. Lilley, M.P. Murphy, Detection of reactive oxygen species-sensitive thiol proteins by redox difference gel electrophoresis, J. Biol. Chem. 282 (2007) 22040–22051, https://doi.org/10.1074/jbc.M703591200.
[80] J.A. Komduur, A.N. Leao, I. Monastyrska, M. Veenhuis, J.A. Kiel, Old yellow enzyme confers resistance of *Hansenula polymorpha* towards allyl alcohol, Curr. Genet. 41 (2002) 401–406, https://doi.org/10.1007/s00294-002-0321-z.
[81] E.W. Trotter, E.J. Collinson, I.W. Dawes, C.M. Grant, Old yellow enzymes protect against acrolein toxicity in the yeast *Saccharomyces cerevisiae*, Appl. Environ. Microbiol. 72 (2006) 4885–4892, https://doi.org/10.1128/aem.00526-06.
[82] E.R. Beynon, Z.C. Symons, R.G. Jackson, A. Lorenz, E.L. Rylott, N.C. Bruce, The role of oxophytodienoate reductases in the detoxification of the explosive 2,4,6-trinitrotoluene by Arabidopsis, Plant Physiol. 151 (2009) 253–261, https://doi.org/10.1104/pp.109.141598.
[83] F. Schaller, C. Biesgen, C. Müssig, T. Altmann, E.W. Weiler, 12-Oxophytodienoate reductase 3 (OPR3) is the isoenzyme involved in jasmonate biosynthesis, Planta 210 (2000) 979–984, https://doi.org/10.1007/s004250050706.
[84] C. Müssig, C. Biesgen, J. Lisso, U. Uwer, E.W. Weiler, T. Altmann, A novel stress-inducible 12-oxophytodienoate reductase from *Arabidopsis thaliana* provides a potential link between Brassinosteroid-action and Jasmonic-acid synthesis, J. Plant Physiol. 157 (2000) 143–152, https://doi.org/10.1016/S0176-1617(00)80184-4.
[85] L. Al-Hijab, A. Gregg, R. Davies, H. Macdonald, M. Ladomery, I. Wilson, Abscisic acid induced a negative geotropic response in dark-incubated *Chlamydomonas reinhardtii*, Sci. Rep. 9 (2019) 12063, , https://doi.org/10.1038/s41598-019-48632-0.
[86] Y. Lu, J. Xu, Phytohormones in microalgae: a new opportunity for microalgal biotechnology? Trends Plant Sci. 20 (2015) 273–282, https://doi.org/10.1016/j.tplants.2015.01.006.
[87] W. Li, B. Liu, L. Yu, D. Feng, H. Wang, J. Wang, Phylogenetic analysis, structural evolution and functional divergence of the 12-oxo-phytodienoate acid reductase gene family in plants, BMC Evol. Biol. 9 (2009) 90, https://doi.org/10.1186/1471-2148-9-90.
[88] G.-Z. Han, Evolution of jasmonate biosynthesis and signaling mechanisms, J. Exp. Bot. 68 (2016) 1323–1331, https://doi.org/10.1093/jxb/erw470.